High resolution near-IR spectroscopy of Arcturus and 10 Leo

Refining a near-IR iron line list

D. T. Andreasen[1,2], S. G. Sousa[1], E. Delgado Mena[1], N. C. Santos[1,2], and T. Lebzelter

[1] Instituto de Astrofísica e Ciências do Espaço, Universidade do Porto, CAUP, Rua das Estrelas, 4150-762 Porto, Portugal e-mail: `daniel.andreasen@astro.up.pt`
[2] Departamento de Física e Astronomia, Faculdade de Ciências, Universidade do Porto, Rua Campo Alegre, 4169-007 Porto, Portugal

ABSTRACT

Context. Effective temperature, surface gravity, and metallicity are basic spectroscopic stellar parameters necessary to characterize a star or a planetary system. Reliable atmospheric parameters for FGK stars have been obtained mostly from methods that relay on high resolution and high signal-to-noise optical spectroscopy. The advent of a new generation of high resolution near-IR spectrographs opens the possibility of using classic spectroscopic methods with high resolution and high signal-to-noise in the NIR spectral window.
Aims. We aim to obtain precise and accurate atmospheric stellar parameters using high quality spectra of two early type K giant stars.
Methods. Our spectroscopic analysis is based on the iron excitation and ionization balance done in LTE.
Results. We get good results!

Key words. data reduction: high resolution spectra – stars individual: Arcturus – stars individual: 10 Leo

1. Introduction

Effective temperature ($T_{\rm eff}$), surface gravity ($\log g$), and metallicity ([M/H], where iron is normally used as a proxy) are fundamental atmospheric parameters necessary to characterise a single star, and to determine other indirect fundamental parameters such as mass, radius, and age from stellar evolutionary models (see e.g. Girardi et al. 2000; Dotter et al. 2008; Baraffe et al. 2015). Precise and accurate stellar parameters are also essential in exoplanet searches. Planetary radius and mass are mainly found from transit lightcurve analysis and radial velocity analysis, respectively. The determination of the mass of the planet implies a knowledge of the stellar mass, while the measurement of the radius of the planet is dependent on our capability to derive the radius of the star (see e.g. Torres et al. 2008; Ammler-von Eiff et al. 2009; Torres et al. 2012).

The derivation of precise stellar atmospheric parameters is not a simple task. Different approaches often lead to discrepant results (see e.g. Santos et al. 2013). Interferometry is usually considered an accurate method for deriving stellar radii (see e.g. Boyajian et al. 2012); however, it is only applicable for bright nearby stars. Asteroseismology, on the other hand, reveals the inner stellar structure by observing the stellar pulsations at the surface. From asteroseismology it is possible to measure the surface gravity and mean density, and therefore to calculate the mass and radius with higher precision (e.g. Kjeldsen & Bedding 1995).

A crucial parameter for the indirect determination of stellar bulk properties is the effective temperature. In that respect, the infrared flux method (IRFM) has proven to be reliable for FGK dwarf and subgiant stars. For higher accuracy the IRFM needs a priori knowledge of the bolometric flux, reddening, surface gravity, and stellar metallicity (Blackwell & Shallis 1977; Ramírez & Meléndez 2005; Casagrande et al. 2010).

Finally, the use of high resolution spectroscopy along with stellar atmospheric models is an extensively tested method that allows the derivation of the fundamental parameters of a star (see e.g. Valenti & Fischer 2005; Santos et al. 2013). The procedure depends on the quality of the spectra, their resolution, and wavelength region. For low resolution spectra ($\lambda/\Delta\lambda < 20\,000$) the preferred method is to fit the overall observed spectrum with a synthetic one (see e.g. Recio-Blanco et al. 2006). Higher resolution spectra of slowly rotating stars (below 10 to 15 km/s) are in the regime where the equivalent width (EW) method can be used (see e.g. **??**, for details).

The derivation of stellar atmospheric parameters from high resolution spectra in the optical is now based on a standard procedure (see e.g. Valenti & Fischer 2005; Sousa et al. 2008). With the advancement of high resolution near-infrared (NIR) instruments, we will now be able to use a similar technique to that used in the optical part of the spectrum (see e.g. Meléndez & Barbuy 1999; Sousa et al. 2008; Tsantaki et al. 2013; Mucciarelli et al. 2013; Bensby et al. 2014). At the moment, the GIANO spectrograph installed at *Telescopio Nazionale Galileo* (TNG) is already available (Origlia et al. 2014), as is the *infrared Doppler instrument* (IRD) installed at the Subaru telescope (Kotani et al. 2014), *Calar Alto high-Resolution search for M dwarfs with Exoearths with Near-infrared and optical Échelle Spectrographs* (CARMENES) for the 3.5 m telescope at Calar Alto Observatory (Quirrenbach et al. 2014), and iShell at the *InfraRed Telescope Facility* (Rayner et al. 2012, 2016). Three new spectrographs are planned for the near future: 1) The *CRyogenic InfraRed Echelle Spectrograph Upgrade Project* (CRIRES+) at the *Very Large Telescope* (VLT) (Follert et al. 2014) with expected first light in 2017, 2) *un SpectroPolarimètre Infra-Rouge A Near-InfraRed Spectropolarimeter* (SPIRou) at *The Canada-France-Hawaii Telescope* (CFHT) (Delfosse et al. 2013; Artigau et al. 2014) with expected first light in 2017 as well, and

3) NIRPS at the ESO 3.6m telescope in La Silla (Conod et al. 2016). The spectral resolutions for these spectrographs range between 50 000 and 100 000.

With the advance of NIR spectrographs, we are yet to be ready for the analysis of the data arriving at the moment and in the future. The analysis of stellar spectra is well understood for FGK stars in the optical part of the spectrum, however some work still needs to be done for the NIR part. Even more challenging are the cold M stars with a severe continuum depression and line blending in the optical.

In this work we analyse the atlas of Arcturus (K0III) and the spectrum of 10 Leo (K1III). The atlas of Arcturus was acquired at Kitt Peak National Observatory using the FTS spectrograph at the Mayall telescope (Hinkle et al. 2003), meanwhile the spectrum of 10 Leo was taken from CRIRES (Nicholls et al. 2016). For the analysis we use the iron line list presented in Andreasen et al. (2016) (referred to as Paper I). This work is a a continuation of our previous work.

The paper is organized as follows. In Sect. 2 we present the data we have acquired for this work along with some information of the two stars we will analyse. in Sect. 3 we refine the iron line list in order to get more reliable stellar parameters. The results are presented in Sect. 4 before we discuss our results in Sect. 5.

2. Data

While the community is currently on the verge to access of a large amount of high resolution NIR spectra with especially the CARMENES spectrographs, the available spectra at the moment are sparse. We chose to use two stars cooler than the Sun since we showed in Paper I that this method works for a star hotter than the Sun (HD 20010).

We have collected the atlas of Arcturus, one of the brightest stars on the Northern hemisphere. Thus it is well studied (see e.g. Griffin & Griffin 1967; McWilliam 1990; Ramírez et al. 2013, to mention just a few). We use the atlas from Hinkle et al. (2003) which covers the spectral range of interest (YJHK bands). Strong telluric features were identified with a spectrum from the TAPAS web page (Bertaux et al. 2014). The atlas also comes with the telluric from a telluric standard and the ratio of the two spectra in order to correct for the tellurics. The telluric spectrum from TAPAS is only used for telluric line identification. We use both the telluric corrected and non-corrected, but note that the telluric correction for Arcturus is not of the same quality as for 10 Leo as described below.

The second spectrum we have achieved is from the CRIRES-POP team (Nicholls et al. 2016). 10 Leo is a very similar star to Arcturus, which is also one reason this star was the first to be fully reduced by the team. The spectrum is divided into each band YJ (only together), H, K, L, and M. We use onlt the first three. It is a great help to be able to compare with the atlas of Arcturus. The main difference is the metallicity of the two stars, since Arcturus is metal poor and 10 Leo has solar metallicity. Some small gaps are present in the spectrum due to tellurics that could not be properly removed, low S/N, bad pixels, etc. Rather than giving an uncertain interpolation, Nicholls et al. (2016) decided to leave small gaps in the data. This have very little effect on this line by line analysis. However, we were unable to measure one Fe ɪɪ line, which are very important to determine the surface gravity.

A small summarise of the data is given in Tab. 1. The data is very similar, with similar S/N which is an approximately value measured with IRAF in the YJ band. The resolutions of the two spectrographs used are the same at 100 000.

Table 1. The star of our two stars with the corresponding spectrograph used to acquire the data and its spectra resolution. In the last column we show the S/N measured with splot in IRAF.

Star	Spectrograph	Resolution	S/N
Arcturus	FTS	100 000	300
10 Leo	CRIRES	100 000	300

In Fig. 1 we compare the spectra of the two stars in a region with some of the iron lines used for the analysis described below.

3. Refining the NIR line list

Besides testing the line list at cooler effective temperatures with two K stars, we also want to refine the line list. This includes identifying recurring outliers (both from the work done in Paper I and in this work), and lines which we are not able to measure, e.g. if a line is amidst a forest of telluric lines. The first step was revisiting the solar atlas used in Paper I. Here 342 Fe ɪ lines and 13 Fe ɪɪ lines were in the process. Most of these were blended with other tellurics while a few were blended with other stellar absorption lines. This procedure leaves us with 84 Fe ɪ lines and 5 Fe ɪɪ lines. This lines should be the best for deploying our technique of determining atmospheric stellar parameters.

The Fe ɪɪ lines are used to determine $\log g$ by imposing ionization balance with Fe ɪ. However, the low number of Fe ɪɪ lines available is a concern, since the average abundance of Fe ɪɪ is affected more by erros, both random and systematic, compared to the Fe ɪ lines. One might fix $\log g$ during the process of obtaining stellar parameters, but this has an impact on the other derived parameters. A more reliable source for $\log g$ could for example be asteroseismology or from the parallaxes measured with GAIA.

During the second look at the Solar spectrum, the EW of the lines were measured by hand (this was done automatically with ARES previously). Since we re-measured the EWs, the log gf values had to be re-calibrated again. Here we simply change the log gf values for the measured EW until the abundance of a given line is equal to that of the Sun, using the same solar atmosphere model as in Paper I. The line list presented here in Appendix **??** is an updated version from Paper I.

4. Results

We derive the stellar atmospheric parameters in the same way as described in Paper I using FASMA (**?**). The EWs are measured for both stars automatically with ARES (Sousa et al. 2015) and by hand with splot in IRAF. We compare the derived stellar parameters from the two measured sets of EWs.

4.1. Arcturus

Arcturus is one of the brightest stars on the night sky with a V magnitude of -0.05 (Ducati 2002). Hence it is a prime target for testing the line list by Paper I with numerous measurements as mentioned above.

The atlas consists of both a summer observation set and a winter observation set. This is in order to minimize the effect of tellurics at different spectral regions. As many lines as possible were measured in both sets. The EW measurements from the different data sets and measurement method (automatic and manual) can be seen in Fig. 2. Parameters were derived from the manual measurements and from the automatic (using both the summer and winter set). For all three sets, parameters were
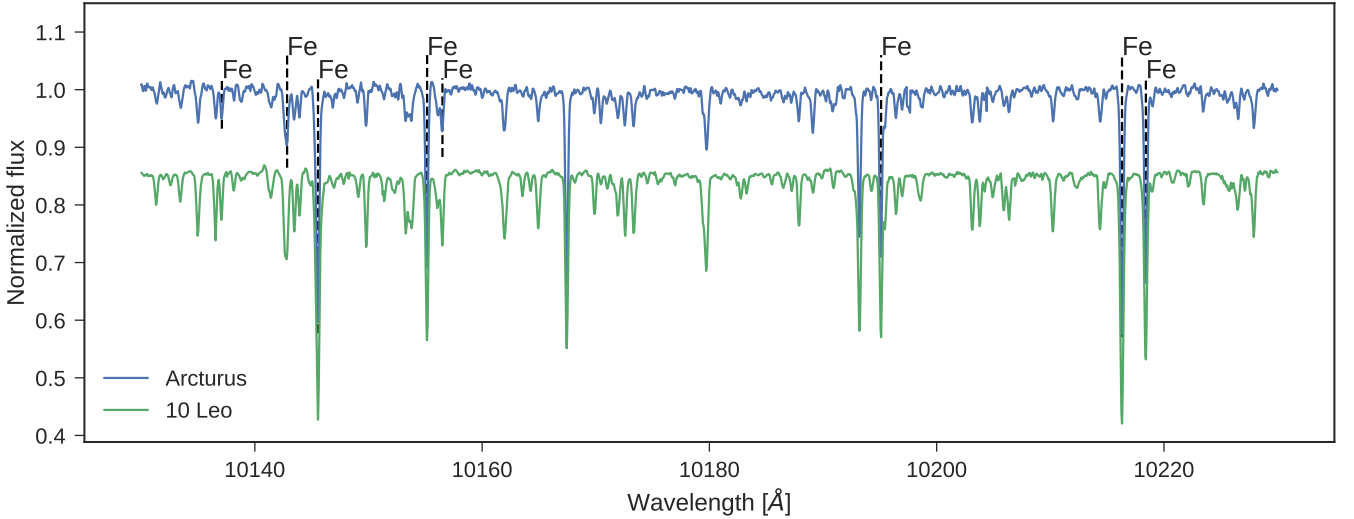
Fig. 1. The spectrum of the two stars, in blue is Arcturus, and green is 10 Leo with an 0.15 offset. We mark the location of Fe I lines in the region.

derived with and without $\log g$ fixed. The derivation follows the procedure presented in Paper I with removal of one outlier iteratively after the minimization routine (**?**) reach convergence. The final results are presented in Tab. 2 with mean parameters from the literature.
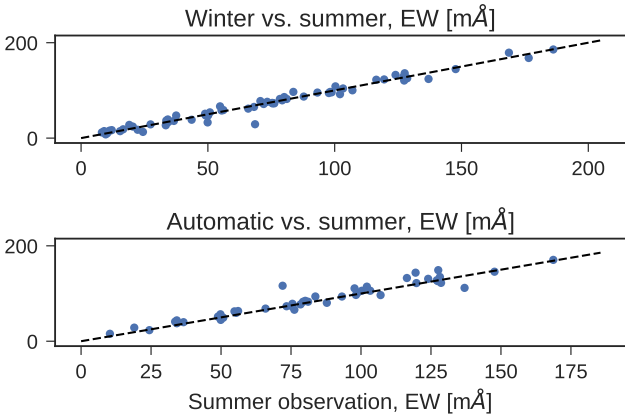

Fig. 2. Top figure: Comparison of the manual EWs measurement between the summer observations and winter observations from the Arcturus spectra. Bottom figure: Same as above, but with automatic measurements from ARES (summer) and manual measurements (summer).

We generally see good agreement between the derived parameters and the values from the literature. The only parameter being difficult to measure is the surface gravity due to the low number of Fe II lines in the NIR. The metallicity is very important to derive accurately, and we report good results overall, but especially with the automatic measurements, compared to literature values. For visualization the parameters are plotted (except ξ_{micro}) in Fig. 3. Here the histogram shows the literature values collected from Simbad while the vertical black line is our final value with gray shaded errorbar.
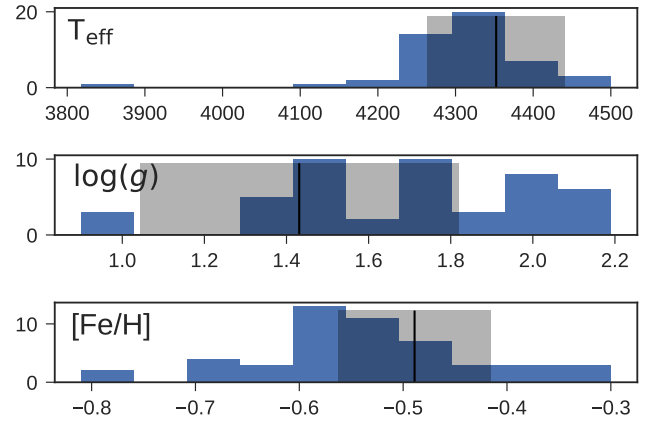

Fig. 3. Histogram of the different sets of literature parameters of Arcturus (except ξ_{micro}). The black vertical line are our derived parameters, and the gray shaded area are the errors on the corresponding parameters.

4.2. 10 Leo

The approach for determining the atmospheric stellar parameters for 10 Leo is identical as for Arcturus. The final reduced data is divided in YJ, H, and K bands. We use ARES on each band separately. For the small gaps in the spectrum, we simply set the flux to 1, since the spectrum is already normalized. This will also prevent ARES to measure any lines in these regions. The EWs from the three regions are combined to one final line list used for the determination of the parameters. The EWs are also measured by hand using IRAF. We list the result in Tab. 3 alongside with a mean of literature values taken from Simbad. The final results and five collected literature values are presented in Fig. 4.

Generally the derived parameters are in excellent agreement with the literature values listed here. Surprisingly we are able to derive good $\log g$ values, although with quite large errors and consistently lower, compared to the results from the literature.

Table 2. The derived parameters for Arcturus with and without fixed surface gravity after 3σ outlier removal. The literature values are a simple mean of all the available parameters on Simbad with the corresponding standard error. There is no microturbulence available, so we derived it using the empirical relation from Adibekyan et al. (2015) for each set of parameters.

	T_{eff} (K)	$\log g$ (dex)	ξ_{micro} (km/s)	[Fe/H] (dex)
Literature	4306 ± 100	1.69 ± 0.32	1.92 ± 0.15	-0.54 ± 0.11
IRAF	4380 ± 79	0.64 ± 0.33	1.14 ± 0.09	-0.49 ± 0.07
IRAF	4212 ± 77	1.69 (fixed)	1.25 ± 0.08	-0.37 ± 0.03
ARES (summer)	4439 ± 63	1.20 ± 0.20	1.55 ± 0.10	-0.58 ± 0.06
ARES (summer)	4348 ± 75	1.69 (fixed)	1.58 ± 0.09	-0.53 ± 0.03
ARES (winter)	4436 ± 67	0.55 ± 1.77	1.35 ± 0.09	-0.56 ± 0.07
ARES (winter)	4233 ± 109	1.69 (fixed)	1.43 ± 0.09	-0.49 ± 0.04
Weighted mean	4421 ± 40	0.96 ± 0.60	1.34 ± 0.05	-0.55 ± 0.04
Weighted mean	4269 ± 51	1.69 (fixed)	1.41 ± 0.05	-0.46 ± 0.02

Table 3. Results from 10 Leo presented in the same way as for Tab. 2 but for 10 Leo.

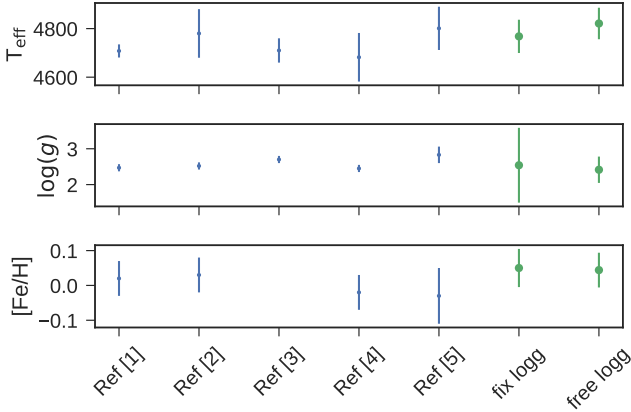|	T_{eff} (K)	$\log g$ (dex)	ξ_{micro} (km/s)	[Fe/H] (dex)
Literature	4720 ± 42	2.54 ± 0.11	1.59 ± 0.02	0.00 ± 0.03
IRAF	4835 ± 85	2.41 ± 0.41	1.28 ± 0.08	0.09 ± 0.06
IRAF	4768 ± 88	2.54 (fixed)	1.20 ± 0.08	0.01 ± 0.05
ARES	4805 ± 98	2.42 ± 0.61	1.23 ± 0.10	-0.01 ± 0.07
ARES	4768 ± 105	2.54 (fixed)	1.20 ± 0.10	-0.01 ± 0.06
Weighted mean	4821 ± 65	2.41 ± 0.37	1.26 ± 0.06	0.04 ± 0.05
Weighted mean	4768 ± 69	2.54 (fixed)	1.20 ± 0.06	0.05 ± 0.04

Fig. 4. Literature values (blue) and the two results from this work (green) with and without $\log g$ fixed. The errorbars on the literature values are wither does presented in the corresponding paper, or in the cases none were presented we give an error of 100 K for T_{eff}, 0.10 dex for $\log g$, and 0.05 for [Fe/H]. References: Ref [1]: Luck (2015), Ref [2]: Park et al. (2013), Ref [3]: Massarotti et al. (2008), Ref [4]: Soubiran et al. (2008), and Ref [5]: da Silva et al. (2011).

5. Discussion

5.1. The role of $\log g$

One of the most difficult atmospheric stellar parameters to get from a spectrum is the surface gravity. Here we need the pressure sensitive ionized atoms such as Fe II. However, they are more sparse than neutral iron, Fe I, making the determination more challenging. This is true in the optical (give ref), and even more in the NIR (see e.g. Paper I and this work). The other three parameters seem to get slightly better when we fix the surface gravity when compared to literature values. With the parallaxes from GAIA (give ref) we will have access to accurate $\log g$, thus

being able to have good T_{eff} and [Fe/H]. We might also see a hint that the method work less well for the most evolved stars (low $\log g$) as Arcturus. The results for 10 Leo, with and without fixed $\log g$, are in agreement within the errorbars. This is not the case for Arcturus for T_{eff} and [Fe/H]. However, these values are all within the errorbars from the literature values. With the coming spectral library by CARMENES (private comm. Amado, P.) we will have dwarf stars to test this method, which is what it is intended for.

5.2. Proper data reduction

In our previous work we had problems getting reliable atmospheric stellar parameters for HD 20010. This was probably because of the unfinished data reduction of from CRIRES-POP at the time. Here the wavelength calibration was done automatically and therefore not optimal. This meant the wavelength was stretched when compared to a synthetic spectrum, which is discussed in more detail by Nicholls et al. (2016). The poor wavelength calibration for HD 20010 most likely caused bad EW measurements. In addition the spectrum was not corrected for telluric lines which also cause minor deviation from the true EW when measured.

All the above problems we had with HD 20010 have been solved for 10 Leo, and it is clear the results are of much higher quality. This can be seen by the smaller errors we have on our parameters, and the good agreement with all parameters compared with the literature. Therefore, it may be needed that a telluric correction is applied to the spectrum before atmospheric stellar parameters can be determined reliably. However, with our limited sample it is hard to make a clear conclusion yet.

6. Conclusion

Being able to successfully determine parameters for two early K giants, we are now making the bridge for the line list towards

cooler temperatures. The obvious next step is the even colder M stars. Particular interesting are the M dwarfs, known to be prone forming rocky planets. As important as cooler stars, we have yet to test our line list on any dwarf stars other than the Sun for which our line list is calibrated. While it is expected that it will work for early dwarf K type stars, it will still be an important accomplishment.

References

Adibekyan, V. Z., Benamati, L., Santos, N. C., et al. 2015, MNRAS, 450, 1900
Ammler-von Eiff, M., Santos, N. C., Sousa, S. G., et al. 2009, A&A, 507, 523
Andreasen, D. T., Sousa, S. G., Delgado Mena, E., et al. 2016, A&A, 585, A143
Artigau, É., Kouach, D., Donati, J.-F., et al. 2014, in Society of Photo-Optical Instrumentation Engineers (SPIE) Conference Series, Vol. 9147, Society of Photo-Optical Instrumentation Engineers (SPIE) Conference Series, 15
Baraffe, I., Homeier, D., Allard, F., & Chabrier, G. 2015, A&A, 577, A42
Bensby, T., Feltzing, S., & Oey, M. S. 2014, A&A, 562, A71
Bertaux, J. L., Lallement, R., Ferron, S., Boonne, C., & Bodichon, R. 2014, A&A, 564, A46
Blackwell, D. E. & Shallis, M. J. 1977, MNRAS, 180, 177
Boyajian, T. S., von Braun, K., van Belle, G., et al. 2012, ApJ, 757, 112
Casagrande, L., Ramírez, I., Meléndez, J., Bessell, M., & Asplund, M. 2010, A&A, 512, A54
Conod, U., Blind, N., Wildi, F., & Pepe, F. 2016, in Proc. SPIE, Vol. 9909, Society of Photo-Optical Instrumentation Engineers (SPIE) Conference Series, 990941
da Silva, R., Milone, A. C., & Reddy, B. E. 2011, A&A, 526, A71
Delfosse, X., Donati, J.-F., Kouach, D., et al. 2013, in SF2A-2013: Proceedings of the Annual meeting of the French Society of Astronomy and Astrophysics, ed. L. Cambresy, F. Martins, E. Nuss, & A. Palacios, 497–508
Dotter, A., Chaboyer, B., Jevremović, D., et al. 2008, ApJS, 178, 89
Ducati, J. R. 2002, VizieR Online Data Catalog, 2237
Follert, R., Dorn, R. J., Oliva, E., et al. 2014, in Society of Photo-Optical Instrumentation Engineers (SPIE) Conference Series, Vol. 9147, Society of Photo-Optical Instrumentation Engineers (SPIE) Conference Series, 19
Girardi, L., Bressan, A., Bertelli, G., & Chiosi, C. 2000, A&A Supp., 141, 371
Griffin, R. & Griffin, R. 1967, MNRAS, 137, 253
Hinkle, K., Wallace, L., Livingston, W., et al. 2003, in Cambridge Workshop on Cool Stars, Stellar Systems, and the Sun, Vol. 12, The Future of Cool-Star Astrophysics: 12th Cambridge Workshop on Cool Stars, Stellar Systems, and the Sun, ed. A. Brown, G. M. Harper, & T. R. Ayres, 851–856
Kjeldsen, H. & Bedding, T. R. 1995, A&A, 293, 87
Kotani, T., Tamura, M., Suto, H., et al. 2014, in Society of Photo-Optical Instrumentation Engineers (SPIE) Conference Series, Vol. 9147, Society of Photo-Optical Instrumentation Engineers (SPIE) Conference Series, 14
Luck, R. E. 2015, AJ, 150, 88
Massarotti, A., Latham, D. W., Stefanik, R. P., & Fogel, J. 2008, AJ, 135, 209
McWilliam, A. 1990, ApJS, 74, 1075
Meléndez, J. & Barbuy, B. 1999, ApJS, 124, 527
Mucciarelli, A., Pancino, E., Lovisi, L., Ferraro, F. R., & Lapenna, E. 2013, ApJ, 766, 78
Nicholls, C. P., Lebzelter, T., Smette, A., et al. 2016, ArXiv e-prints [e-prints[arXiv]1609.07873]
Origlia, L., Oliva, E., Baffa, C., et al. 2014, in Society of Photo-Optical Instrumentation Engineers (SPIE) Conference Series, Vol. 9147, Society of Photo-Optical Instrumentation Engineers (SPIE) Conference Series, 1
Park, S., Kang, W., Lee, J.-E., & Lee, S.-G. 2013, AJ, 146, 73
Quirrenbach, A., Amado, P. J., Caballero, J. A., et al. 2014, in Society of Photo-Optical Instrumentation Engineers (SPIE) Conference Series, Vol. 9147, Society of Photo-Optical Instrumentation Engineers (SPIE) Conference Series, 1
Ramírez, I., Allende Prieto, C., & Lambert, D. L. 2013, ApJ, 764, 78
Ramírez, I. & Meléndez, J. 2005, ApJ, 626, 446
Rayner, J., Bond, T., Bonnet, M., et al. 2012, in Proc. SPIE, Vol. 8446, Ground-based and Airborne Instrumentation for Astronomy IV, 84462C
Rayner, J., Tokunaga, A., Jaffe, D., et al. 2016, in Proc. SPIE, Vol. 9908, Society of Photo-Optical Instrumentation Engineers (SPIE) Conference Series, 990884
Recio-Blanco, A., Bijaoui, A., & de Laverny, P. 2006, MNRAS, 370, 141
Santos, N. C., Sousa, S. G., Mortier, A., et al. 2013, A&A, 556, A150
Soubiran, C., Bienaymé, O., Mishenina, T. V., & Kovtyukh, V. V. 2008, A&A, 480, 91
Sousa, S. G., Santos, N. C., Adibekyan, V., Delgado-Mena, E., & Israelian, G. 2015, A&A, 577, A67
Sousa, S. G., Santos, N. C., Mayor, M., et al. 2008, A&A, 487, 373
Torres, G., Fischer, D. A., Sozzetti, A., et al. 2012, ApJ, 757, 161
Torres, G., Winn, J. N., & Holman, M. J. 2008, ApJ, 677, 1324
Tsantaki, M., Sousa, S. G., Adibekyan, V. Z., et al. 2013, A&A, 555, A150
Valenti, J. A. & Fischer, D. A. 2005, ApJS, 159, 141